CRYSTAL GROWTH & DESIGN
Article
pubs.acs.org/crystal

Crystals and Aggregates of a Molecular Tetrarotor with Multiple Trityl Embraces Derived from Tetraphenyladamantane

Antoine Stopin and Miguel A. Garcia-Garibay*

Department of Chemistry and Biochemistry, University of California, Los Angeles, Los Angeles, California 90095, United States

Supporting Information

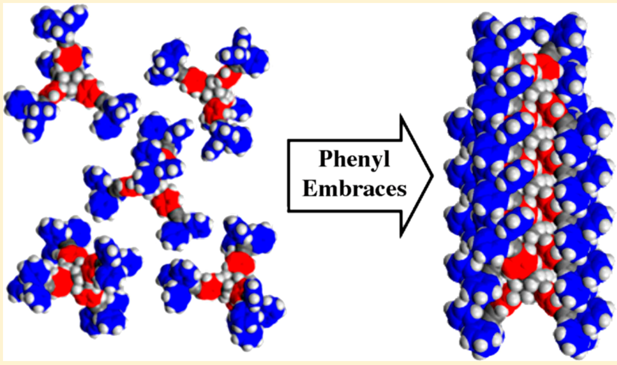

ABSTRACT: Samples of tetrakis-1,3,5,7-(4′-(3″,3″,3″-triphenylpropynyl)-phenylene)adamantane and its trityl-deuterated isotopologue were synthesized and their crystallization and packing properties were analyzed within the context of formation of 4- or 6-fold phenyl embraces. The tetrahedral shape of these molecules with four propeller-like triphenylmethyl moieties generates several edge-to-face intermolecular interactions in the solid state that result in the formation of infinite chains of molecules that are tightly interlocked. The formation of analogous edge-to-face intermolecular interactions leading to aggregation in solution was also suggested by NMR experiments carried out in different solvents as a function of concentration. The formation of interdigitated chains was also manifested in fibrils and thin needles, which were documented by scanning electron microscopy (SEM). Single crystal X-ray diffraction studies revealed the presence of multiple 4-fold phenyl embraces and edge-to-face interactions as the leading motifs behind the formation of tightly interlocked molecular chains.

■ INTRODUCTION

Over the past few years we have been interested in low-density molecular crystals built with molecules that pack poorly and generate some free volume in order to facilitate internal rotation in the solid state. The most general and successful motif in our studies consists of a small central rotator axially linked to bulky shielding groups that act as the stator (Figure 1). We have analyzed compounds with bridging groups across the two ends of the structure, which are analogous to macroscopic toy gyroscopes (Figure 1a, left), and structures with open topologies, such as 1,4-bis(3,3,3-triphenylpropinyl)-benzene (Figure 1, right), which have a dumbbell-shaped structure.

It is well-known that dumbbell-shaped molecules have poor shape complementarity and tend to form solvates that are often referred to as "wheel-and-axle" complexes.[1−3] Soldatov[4] noted that low density crystals are generally formed by structures that lack complementary contacts for all of their surfaces,[5] which encompasses, among others, bulky shapes penetrated by a rod[6−8] and bulky structures interconnected by several rods.[9,10] As illustrated in Figure 1b, we have shown that the crystallization of compounds with triphenylmethyl stators and a diethynyl-arylene or diethynyl-cycloalkylidene rod tend to occur in a remarkably reliable manner in the form of parallel chains of molecular rotors interacting at both ends by complementary edge-to-face interactions characteristic of the well-known 6-fold phenyl embrace (6PE).[11] The 6PE is characterized by a cyclic arrangement of complementary edge-to-face interactions between adjacent Ph_3X groups (XPh_3----Ph_3X). Their structures may differ by their local symmetry, which may have a point group as high as S_6, and by the number of geometrically different nearest neighbors (I, II, etc.). Other differences include their rotators' centroid-to-centroid distances (m_1), the distances between molecules in neighboring chains (d_1), and the displacement distances along the chain direction between molecules in neighboring chains (d_2). Structures analyzed in our group that conform to the motif in Figure 1b include triphenylmethyl stators with a simple diyne rod,[12] with various diethynyl substituted phenylenes (H, NH_2, CN, NO_2, F, F_2, NH_2/NO_2),[13] diphenylethynyl-diamantane,[14] diethynyl biphenylene,[15] with diethynyl pyridine, pyridazine, and pyridine N-oxide,[16] as well as triphenylsilyl stators with diethynyl phenylene, cubanediyl, bicyclo[2.2.2]-octanediyl, *para*-closo-dicarba-dodecacarboranediyl.[17] Having shown that the 6PE is a robust crystal engineering synthon[18] for linear structures, we were interested to see whether it would be sufficiently strong to help direct a three-dimensional noncovalent network. To answer this question we prepared and analyzed molecular tetrarotor **1** with one adamantane group at the core and four triphenylmethyl groups linked by *para*-ethynylene-phenylene rods arranged in a tetrahedral arrangement (Figure 2). In principle, the linear nature of the 6PE combined with the tetrahedral structure and extended trityl branches of compound **1** could give rise to an

Received: May 9, 2012
Revised: June 5, 2012
Published: June 11, 2012

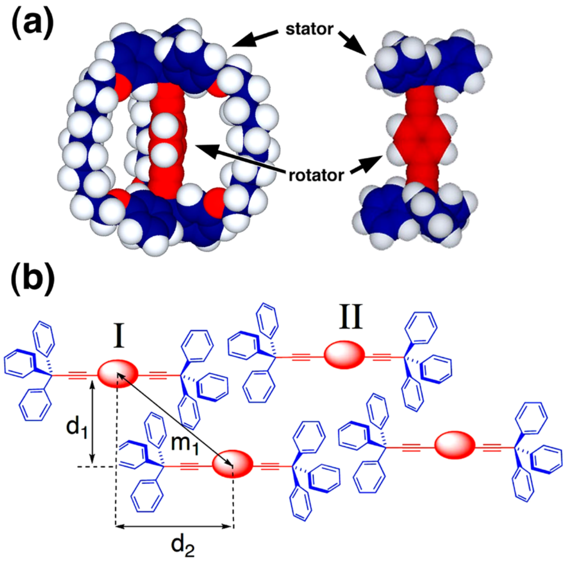

Figure 1. (a) Molecular rotors with triply bridged, closed topologies, analogous to those of macroscopic gyroscopes (left), and structures with open topologies (right) tend to form crystals that generate sufficient free volume for fast rotation of the central phenylene rotator. (b) The packing of molecular rotors with triphenylmethyl stators is dictated by aromatic edge-to-face interactions in the form of a self-complementary 6-fold phenyl embraces (6PEs).

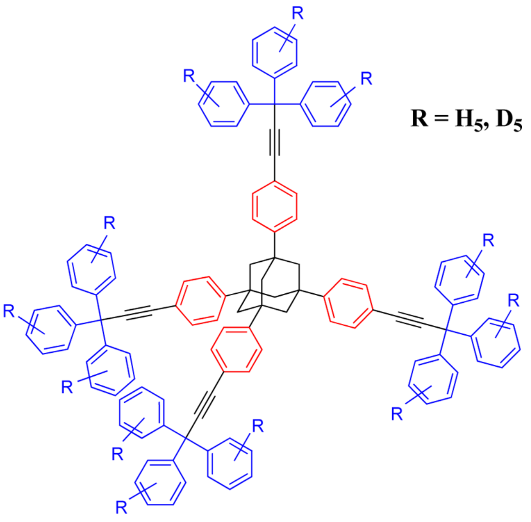

1, 1-d_{60}

Figure 2. Tetrakis-1,3,5,7-(4′-(3″,3″,3″-triphenylpropynyl)-phenylene)-adamantane molecular tetrarotors **1** and **1**-d_{60}.

interpenetrated diamond lattice. In contrast, aromatic edge-to-face interactions with lower symmetry would give rise to lower symmetry packing structures.

With the purpose of probing the presence of aromatic interactions in solution using ^{1}H and ^{2}H NMR in a variety of deuterated and non-deuterated solvents, we prepared compound **1** in its natural abundance and trityl-deuterated forms (**1**-d_{60}, Scheme 1). We wanted to investigate whether the edge-to-face interactions that tend to occur in the solid state, would be present in solution, potentially resulting in anisotropic shielding effects that could be observed in the form of concentration-dependent chemical shifts, and/or by changing the characteristics of the solvent using mixtures of good and bad solvents. We set out to test whether compound **1** would crystallize with ease, form an open structure, and display aromatic edge-to-face interactions in the form of 6-fold (6PE) or 4-fold phenyl embraces (4PE). We report here our crystallization studies in multiple solvents showing the formation of thin needles and the formation of a “gel-like” structure. We describe the experimental conditions required to grow diffraction-quality single crystals and the resulting X-ray molecular and crystal structures. We analyze how the packing structure of **1** is remarkably dense and can be described in terms of infinite chains of molecules experiencing complementary aromatic edge-to-face interaction involving the trityl groups at the periphery and the phenyl groups attached to the adamantyl core.

■ RESULTS AND DISCUSSION

Synthesis and Characterization. The adamantyl tetrarotor **1** was synthesized from trityl chloride **2** and tetraphenyl adamantane **4** as illustrated in Scheme 1. The deuterated trityl chloride **2**-d_{15} was obtained by a Friedel–Crafts reaction of deuterated benzene and carbon tetrachloride. Compounds **3** and **3**-d_{15} were obtained in one step, respectively, by reaction of **2** and **2**-d_{15} with ethynylmagnesium bromide in benzene.[15] Tetra-*p*-iodophenyl adamantane **5** was obtained in 69% yield by iodination of tetraphenyl adamantane **4** using [bis-(trifluoroacetoxy)iodo]benzene.[19] Molecular tetrarotors **1** and **1**-d_{60} were obtained via Sonogashira coupling of **5** with the corresponding trityl acetylene. The structures of compound **1** and **1**-d_{60} were confirmed by ^{1}H, ^{2}H, and ^{13}C NMR, attenuated total reflectance (ATR) FTIR, and by mass spectrometry.

The ^{1}H NMR spectra of **1** and **1**-d_{60} showed a broad singlet at 2.15 ppm characteristic of the adamantane methylene hydrogens, the four phenyl groups linked to the adamantane present the characteristic AA′BB′ spin system of *para*-disubstituted benzene as two apparent doublets between 7.40 and 7.55 ppm. The ^{1}H NMR spectrum of **1**-d_{60} shows weak signals between δ 7.28 and δ 7.38 due to residual hydrogens in the starting material, while stronger signals can be seen for compound **1** due to the triphenylmethyl groups. As expected, the ^{13}C NMR spectra of **1** and **1**-d_{60} are very similar with two alkyne signals at ca. 85 and 95 ppm, a quaternary trityl carbon at ca. 56 ppm, and adamantane signals at ca. 39 and 47 ppm. Strong signals at ca. 121, 125, 132, and 149 ppm in both ^{13}C NMR spectra correspond to the phenyl groups linked to the adamantane. The triphenylmethyl groups for both compounds present a signal at ca. 145 ppm corresponding to the ipso-carbon. The other carbons of the trityl groups can be seen as three singlets between 126 and 129 ppm for compound **1**, but they appear as three multiplets in the same range for **1**-d_{60} due to the carbon-deuterium coupling. The IR spectrum of compound **1**-d_{60} displays a signal at ca. 2275 cm^{-1} corresponding to the stretching of the carbon–deuterium bonds. Visual melting point observations indicated that compounds **1** and **1**-d_{60} decompose before melting above 400 °C. The molecular ions of the two isotopologues were observed by mass spectrometry and conformed well with the expectations based on the respective molecular masses.

Crystallization Studies. The crystallization of compound **1** was investigated in different solvent systems. A large number of trials showed indistinguishable behavior of compounds **1** and **1**-d_{60}. The solvents used for these tests were determined by the relatively low solubility of **1**, which is high in tetrahydrofuran (THF), dichloromethane (DCM), and chloroform but low in

Scheme 1

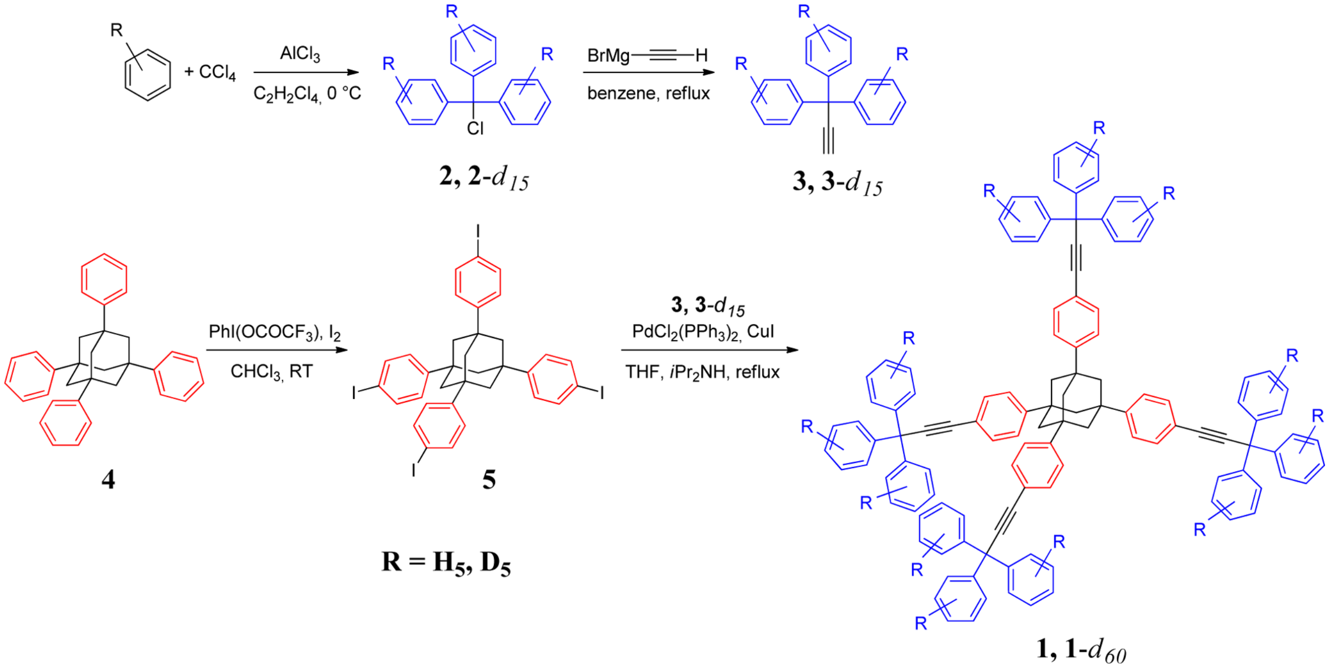

most other solvents. Slow evaporation of a DCM solution of compound **1** yielded very thin needles that were too small to obtain a crystal structure. Similar results were obtained upon addition of other poor solvents such as benzene, methanol, ethyl acetate, or toluene. Similar results were also obtained by slow evaporation of a solution of **1** in chloroform or THF in the presence of toluene. Tests were also carried out by slow diffusion of various solvents into a solution of **1** in DCM, chloroform, or THF. Once again, the needles formed were too small for single crystal X-ray diffraction analysis.

Crystallizations were also tested by slow diffusion of methanol toward a concentrated solution of **1** in THF. Under these conditions, the formation of needles occurred at the interface of the two solvents. Further experiments involving the fast addition of methanol into a solution of compound **1** in tetrahydrofuran resulted in the formation of a suspension that settles with time and takes the appearance of a weak gel after removal of the excess solvent. This behavior suggested the formation of nanofibers as a result of nonbonding interactions between molecules of **1**.

Aggregation in Solution Studied by ^{1}H and ^{2}H NMR. We speculated that 6-fold (6PE) and 4-fold (4PE) trityl embraces involving aromatic edge-to-face interacions, if present in solution, should result in chemical shift displacements of the aromatic trityl protons due to the anisotropic field effects of the interacting π-systems.[20] To explore this, compound **1** was dissolved in deuterated THF (5 mg in 0.5 mL) and deuterated methanol was then added in small portions (50 μL). A shift of the aromatic protons observed upon addition of methanol was correlated with a change in the chemical shift of the adamantyl aliphatic hydrogens and was interpreted as an indication of the change in solvent properties rather than to aggregation effects. After addition of 300 μL of methanol, the sample began to cloud and precipitate with the concomitant broadening of the aromatic proton signals. Analogous experiments using deuterium NMR with samples of **1**-d_{60} in natural abundance THF with the subsequent slow addition of methanol gave similar results. However, support for a rather weak aggregate in solution was obtained from a series of ^{1}H NMR spectra of **1**-d_{60} acquired at 500 MHz in THF-d_8 as a function of concentration with samples that varied from 2.5 mM up to 26 mM, which is close to the solubility limit. Taking the signal of the adamantyl methylene hydrogens as an internal standard, we were able to determine the displacement of the sharp residual hydrogens of the deuterated trityl groups with accuracy to look for concentration-dependent field effects on their chemical shifts. We detected small but characteristic upfield chemical shift changes in these signals of up to 2.00 ± 0.05 Hz and 3.00 ± 0.05 Hz for the *ortho*- and *para*-phenyl trityl hydrogens, respectively, and a downfield shift of 2.00 ± 0.05 Hz for the *meta*-hydrogens. Signals corresponding to the *para*-phenylene rotators attached to the adamantyl group also displayed upfield and downfield shifts of 1.80 ± 0.05 and 0.50 ± 0.05 Hz, respectively. Considering that the edge-to-face-interactions characteristic of a 6-fold trityl embraces should result in shielding effects for all the edge-on aromatic hydrogens, we tentatively suggest that analogous aggregates with multiple types aromatic interactions are formed also in solution (see Supporting Information).

Scanning Electron Microscopy (SEM). The results observed upon crystallization of **1** under two representative conditions were analyzed by scanning electron microscopy (SEM). These included the formation of thin single needles and a suspension at the interface of slowly diffusing methanol into a concentrated solution of **1** in THF and the formation of a weak "gel-like" system upon fast addition of a solution of **1** in THF to methanol followed by removal of the excess solvent. Samples were deposited from their respective solutions onto a silicon wafer (1.0.0) previously treated with a piranha solution consisting of mixture of water, hydrochloric acid, and hydrogen peroxide under reflux, in order to obtain a smooth surface. The silicon wafers were dried under a slow flow of argon and placed in a desiccator overnight before SEM analysis.

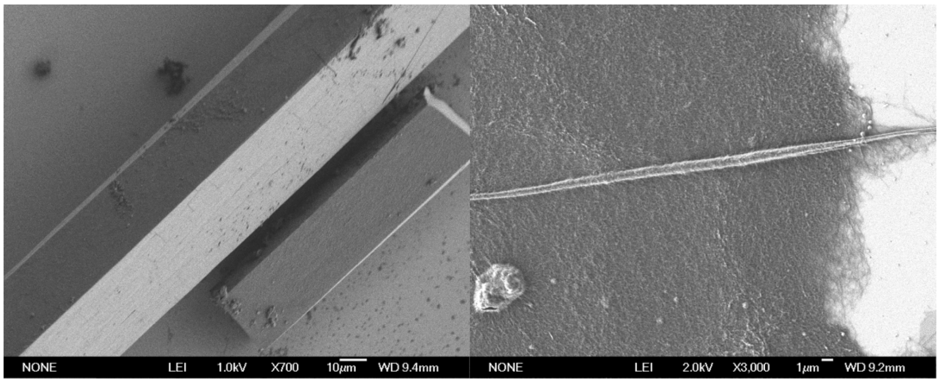

Figure 3. SEM pictures of compound **1** obtained (left) by slow diffusion of methanol into a concentrated solution of **1** in THF and (right) by addition of methanol into a concentrated solution of **1** in THF.

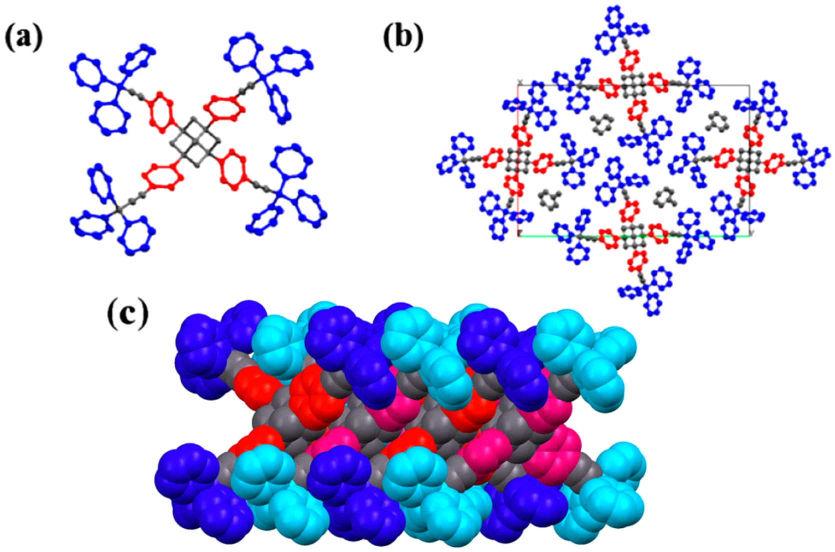

Figure 4. Views from the molecular and crystal structure of **1** at 100 K. (a) Molecular structure with thermal ellipsoids at 50% probability, (b) unit cell along the *c*-axis with solvent included, and, (c) space-filling representation of the packing structure illustrating the formation of linear chains of interlocking molecules along the *c*-axis (left to right). Hydrogen atoms are omitted and molecules in the chain are illustrated in alternating dark and light colors.

The needles obtained by slow nucleation were between ca. 10 to 30 μm wide and several hundreds of micrometers long (Figure 3 left). These needles presented rectangular cross sections with sharp edges and were found to be very brittle when exposed to external forces. The suspension that appeared at the interface of THF and methanol consisted of very thin needles, between 1 to 15 μm wide (Figure 3 right) with excess of the compound precipitated in the form of fibrils. The presence of thin needles or aggregates over three different scales suggested to us the formation of a dominant one-dimensional close packing array. In agreement with this suggestion, the rapidly precipitated "gel-like" samples were shown to consist of similar fibrils and thin needles.

Single Crystal X-ray Diffraction Analysis. X-ray quality single crystalline needles slightly larger than those obtained from THF-MeOH were obtained by slow evaporation of a solution of compound **1** in pure toluene. The X-ray crystallographic data were collected at 100 K with a crystal of **1**,[21] and the structure was solved in the chiral orthorhombic space group $P2_12_12$ with one-half molecule of **1** and one molecule of toluene per asymmetric unit. The unit cell contains two molecules of compound **1** and four molecules of toluene. A depiction of the unit cell is shown in Figure 4 with four molecules each of **1** and toluene. Notably, compound **1** crystallizes with a structure in the point group S_4 with triphenylmethyl groups having different propeller chiralities, P and M. The two crystallographically different alkynyl axles present in the molecule are slightly bent, with angles C10−C13−C14 of 174.6° and C37−C40−C41 of 173.3°. The phenylene groups directly linked to the adamantane unit are eclipsed with one of the three adamantyl $C_{quat}-CH_2$ bonds, and the C−Ph bonds of the trityl groups are in a staggered conformation with respect to the three $C_{quat}-CH_2$ bonds coming out of the adamantane core.

The crystal structure of **1** has a packing coefficient of 0.733, which falls in the range of 0.65−0.77 typically observed for molecular crystals. The unit cell dimensions are 20.994 Å, 32.153 Å, and 6.953 Å, with the smaller *c*-axis being the direction of the interdigitated triphenyl propynyl chains that experience two types of phenyl embraces.[22] As shown in Figure 4c, the packing structure may be described in terms of infinite chains of interlocking molecules that translate along the direction of the *c*-axis. The crystal structure of **1** shows multiple edge-to-face interactions involving the phenyl groups

Table 1. Geometric Parameters Involved in the Four-Fold Phenyl Embrace (4PE) Illustrated in Figure 6[a]

$\pi_{edge} \rightarrow \pi_{face}$	contact	$\pi \cdots \pi$ (Å)	$H \cdots \pi$ (Å)	$C{-}H \cdots \pi$ (°)	ϕ (°)
$II_D \rightarrow I_A$ /I $I_B \rightarrow I_C$	$C12{-}H12 \cdots \pi_5$[a]	5.255	3.156	146.7	75.9
$I_A \rightarrow II_B$ / $I_C \rightarrow II_D$	$C39{-}H39 \cdots \pi_1$[b]	4.975	2.851	148.3	78.6

[a] Symmetry codes: (a) $-x, -y + 1, z - 1$; (b) $x, y, z + 1$.

attached to the adamantane at the core and the phenyl groups of the peripheral trityl moieties. Aromatic edge-to-face interactions were identified by searching for close distances among the aromatic C−H bonds and the π-ring centroids of the phenyl and phenylene rings in the structure.[23] Notably, two sets of such interactions were identified. One involves only the phenyl groups attached to the adamantane core, and the second involves one of the adamantyl phenyls with three more phenyl groups from the outer trityls. The first set is reported in Table 1 and shown schematically in Figure 5 with edge-to-face interactions highlighted with green arrows. Included in the table are the centroid-to-centroid distances below 5.3 Å, the associated C−H···π distances, the C−H···π angles between the C−H bond vector and a vector drawn from the aromatic hydrogen to the centroid of the ring, and the angle Φ, formed between the plane of the aromatic ring and the projection of the C−H vector to the plane of aromatic ring. It should be noted that idealized edge-to-face, or T-interactions would have a π-centroid-to-π-centroid distance of ca. 5 Å, a C−H···π angle of 90°, and an angle Φ = 180°. It is well-known however that the corresponding potential is relatively soft and large variations on these parameters are frequently observed. Analyzed closely, the interaction in Figure 5 constitutes an asymmetric 4-fold phenyl embrace similar to the one described by Boldog and coworkers for the 1,3,5,7-tetraphenyladamantane, with two phenyl groups from each side of the embracing molecules involved in interactions along the two directions of the chain.[24] The interaction is not symmetric as it pertains to the roles of the phenyl groups involved in the edge-to-face interactions, as illustrated schematically in the top of Figure 5 with aromatic rings labeled A−D and the arrows indicating the direction of the C−H···π vector. Interactions occur in a cyclic manner between the edge of ring A and the face of ring B, the edge of B and the face of C, the edge of C and the face of D, closing the cycle with the edge of D and the face of A. Rings A and C are related by a 2-fold symmetric axis and are crystallographically nonequivalent to rings B and D, which are symmetrically related to each other.

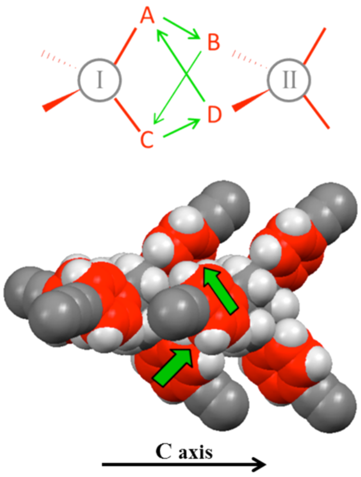

Figure 5. Four-fold phenyl embrace involving four phenyl groups linked to two different adamantyl moieties shown in a schematic manner and in a space-filling model (parts of the molecules not involved in the phenyl embraces were omitted for clarity).

Shown in Figure 6 with a sketch that defines the notation used below is the second set of “distorted” 4-fold phenyl embraces that can be identified. These involve one phenyl group linked to the adamantyl moieties (labeled α and shown in red), one phenyl ring from a trityl group within the same molecule (labeled γ, in blue), and two from an adjacent molecule along the chain (labeled β and γ, also in blue). As indicated by the green arrows in the figure, the cyclic array in this case follows a connectivity that goes from the edge of ring α the face of ring β, from the edge of β to the face of γ, from the edge of γ to the face of δ, with the cycle closing from the edge of δ to the face of α. The geometric features of these interactions, which are all distinct, are documented numerically in Table 2.

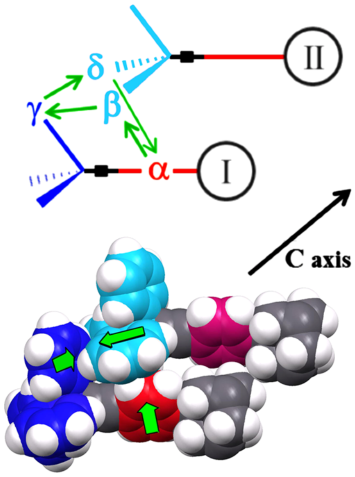

Figure 6. Distorted 4-fold phenyl embrace (4PE) including phenyl rings attached to the adamantyl and trityl groups of two neighbors along the chain shown in a schematic manner and in a space-filling model (parts of the molecules were omitted for clarity).

The interaction in Figure 6 can be viewed as analogous to the one present in tetraphenylmethane, with one of the rings containing an acetylene group that acts as an extender and distorts the symmetry of the molecule. It is notable that no specific interactions appear to exist between trityl groups in adjacent chains, indicating that the intermolecular 6-fold phenyl embrace may not be sufficiently strong to dictate the formation of extended tetrahedral networks.

■ CONCLUSIONS

We have prepared samples of tetrakis-1,3,5,7-(4′-(3″,3″,3″-triphenylpropynyl)-phenylene)adamantane **1** and its deuterated analogue **1**-d_{60} and characterized their crystallization behavior in order to evaluate the formation of 6-fold and 4-fold phenyl

Table 2. Geometric Parameters Involved in the Four-Fold Phenyl Embrace Illustrated in Figure 6[a]

$\pi_{edge} \rightarrow \pi_{face}$	contact	$\pi \cdots \pi$ (Å)	$H \cdots \pi$ (Å)	$C-H \cdots \pi$ (°)	ϕ (°)
$I\alpha \rightarrow II\beta$	$C9-H9 \cdots \pi_2{}^b$	4.674	2.655	139.6	79.6
$II\beta \rightarrow I\gamma$	$C20-H20 \cdots \pi_3{}^c$	4.882	2.979	133.8	82.3
$I\gamma \rightarrow II\delta$	$C27-H27 \cdots \pi_4{}^b$	5.131	3.462	123.9	71.9
$II\delta \rightarrow I\alpha$	$C33-H33 \cdots \pi_1{}^c$	4.955	3.037	134.9	77.8
$I\alpha' \rightarrow II\beta'$	$C36-H36 \cdots \pi_6{}^c$	4.602	2.799	127.9	80.1
$II\beta' \rightarrow I\gamma'$	$C47-H47 \cdots \pi_8{}^b$	5.201	3.299	134.3	75.7
$I\gamma' \rightarrow II\delta'$	$C60-H60 \cdots \pi_7{}^c$	5.522	3.744	129.9	65.8
$II_{\delta}' \rightarrow I_{\alpha}'$	$C50-H50 \cdots \pi_5{}^b$	4.421	2.996	112.5	79.5

[a] Symmetry codes: (b) $x, y, z + 1$; (c) $x, y, z - 1$.

embraces. Crystallization studies revealed the formation of ultrathin fibrils that form a "gel-like" network, and long brittle needles with well-developed edges and rectangular cross sections. Both were analyzed by scanning electron microscopy. Single crystal X-ray diffraction analysis of compound **1** confirmed the presence of two distinct 4-fold phenyl embraces with a range of edge-to-face interactions that lead to the formation of infinite molecular chains in a relatively close-packed crystal structure. Weak intermolecular interactions detected in solution as a function of concentration by ^1H NMR and a packing structure with multiple phenyl embraces confirm that these interactions are ubiquitous and important but perhaps not sufficiently strong to direct the packing motif by themselves.

EXPERIMENTAL SECTION

Compounds **2**-d_{15}, **3**, **3**-d_{15}, and **5** were synthesized following reported procedures. All commercial chemicals were used without further purification. THF was distilled over sodium and benzophenone. ^1H and ^{13}C NMR spectra were acquired in $CDCl_3$ respectively at 500 and 125 MHz on a Brüker spectrometer. NMR chemical shifts are reported in parts per million (ppm) relative to the residual peak of the solvent ($CDCl_3$: ^1H $\delta = 7.26$ ppm; ^{13}C $\delta = 77.16$ ppm). Multiplicity is abbreviated to s (singlet), d (doublet), m (multiplet), br (broad), and app (apparent). ^2H NMR were acquired in natural abundance solvents at 77 MHz. IR spectra were recorded on a Perkin-Elmer ATR-FTIR instrument. Decomposition temperatures were determined using a standard melting point apparatus. Mass spectra were acquired on an Agilent 6210 LCMS system. The X-ray crystal structure was acquired at 100 K on a Bruker Smart 1000K diffractometer. SEM pictures were obtained using a JEOL JSM-6700F FE-SEM microscope.

Tetrakis-1,3,5,7-(4′-(3″,3″,3″-triphenylpropynyl)-phenylene)adamantane (1). In a 50-mL three-neck round-bottom flask were added 5 mL of distilled THF and 5 mL of diisopropylamine and the solvents were degassed for 30 min with argon. Compound **3** (100 mg, 0.36 mmol), compound **5** (58 mg, 0.06 mmol), bis(triphenylphosphine)palladium(II) dichloride (4 mg, 0.006 mmol), and copper(I) iodide (1.2 mg, 0.006 mmol) were added and the mixture was refluxed for 2 days under argon. The reaction mixture was then washed with 5 mL of saturated ammonium chloride solution and then extracted with DCM (20 mL then 2 × 10 mL). The organic phases were then combined, washed successively with water (5 mL) and brine (5 mL), dried over magnesium sulfate and the solvent was evaporated. The crude product was purified by precipitation of the desired compound by slow evaporation of a solution of **1** in a mixture DCM/hexanes to afford 55 mg of compound **1** as a white powder (60% yield). mp dec >400 °C. ^1H NMR (500 MHz, $CDCl_3$): δ 7.50 (app d, 8H, $J = 8.3$ Hz), 7.41 (app d, 8H, $J = 8.3$ Hz), 7.34−7.24 (m, 60H), 2.12 (br s, 12H); ^{13}C NMR (125 MHz, $CDCl_3$): δ 149.13, 145.52, 131.88, 129.34, 128.15, 126.96, 125.10, 121.71, 95.68, 85.07, 56.26, 47.02, 39.43; FTIR (solid HATR, cm^{-1}): 3058, 3024, 2922, 2852, 1596, 1504, 1490, 1446, 1031, 1026, 842, 834, 758, 740, 726, 695; HRMS $C_{118}H_{89}$ $[M + H^+]$ calcd 1505.6959; found 1505.6900

Tetrakis-1,3,5,7-(4′-(3″,3″,3″-triphenylpropynyl)-phenylene)adamantane (1-d_{60}). In a 100-mL three-neck round-bottom flask were added 25 mL of distilled THF and 25 mL of diisopropylamine and the solvents were degassed for 1 h with argon. Compound **3**-d_{15} (540 mg, 1.9 mmol), compound **5** (300 mg, 0.32 mmol), bis(triphenylphosphine)palladium(II) dichloride (22 mg, 0.031 mmol), and copper(I) iodide (6 mg, 0.032 mmol) were added and the mixture was refluxed for 2 days under argon. The reaction mixture was then washed with 25 mL of saturated ammonium chloride solution and then extracted with DCM (50 mL then 2 × 25 mL). The organic phases were then combined, washed successively with water (25 mL) and brine (25 mL), dried over magnesium sulfate, and the solvent was evaporated. The crude product was purified by silica gel column chromatography (DCM/hexanes: 5:95 to 25:75) to afford 358 mg of compound **1**-d_{60} as a white powder (72% yield). mp dec > 400 °C. ^1H NMR (500 MHz, $CDCl_3$): δ 7.55 (app d, 8H, $J = 8.4$ Hz), 7.46 (app d, 8H, $J = 8.4$ Hz), 2.16 (br s, 12H); ^{13}C NMR (125 MHz, $CDCl_3$): δ 149.12, 145.37, 131.88, 129.07 (m), 127.63 (m), 126.45 (m), 125.09, 121.72, 95.68, 85.00, 56.08, 47.01, 39.42; FTIR (solid HATR, cm^{-1}): 3032, 2923, 2849, 2275, 1560, 1507, 1361, 1329, 1020, 904, 865, 838, 827; HRMS $C_{118}H_{29}D_{60}$ $[M + H^+]$ calcd 1566.0725; found 1566.0725.

ASSOCIATED CONTENT

Supporting Information

FTIR, ^1H and ^{13}C NMR spectra of compounds **1** and **1**-d_{60}. This material is available free of charge via the Internet at http://pubs.acs.org.

AUTHOR INFORMATION

Corresponding Author

*E-mail: mgg@chem.ucla.edu.

Notes

The authors declare no competing financial interest.

ACKNOWLEDGMENTS

We thank the National Science Foundation for support through Grant DMR1101934.

REFERENCES

(1) Toda, F.; Akagi, K. *Tetrahedron Lett.* **1968**, *9*, 3695−3698.

(2) Toda, F.; Ward, D. L.; Hart, H. *Tetrahedron Lett.* **1981**, *22*, 3865−3868.

(3) Hart, H.; Lin, L. T. W.; Ward, D. L. *J. Am. Chem. Soc.* **1984**, *106*, 4043−4045.

(4) Soldatov, D. V. *J. Chem. Cryst.* **2006**, *36*, 747−768.

(5) Host−guest interactions have also been exploited to create low-density and/or solvent inclusion crystalline solids. For recent advances see (a) Ashmore, J.; Bishop, R.; Craig, D. C.; Scudder, M. L. *Cryst. Growth Des.* **2007**, *7*, 47−55. (b) Rahman, A. N. M. M.; Bishop, R.; Craig, D. C.; Scudder, M. L. *Org. Biomol. Chem.* **2004**, *2*, 175−182. (c) Maly, K. E.; Gagnon, E.; Maris, T.; Wuest, J. D. *J. Am. Chem. Soc.* **2007**, *129*, 4306−4322. (d) Trolliet, C.; Poulet, G.; Tuel, A.; Wuest, J. D.; Sautet, P. *J. Am. Chem. Soc.* **2007**, *129*, 3621−3626.

(6) Jetti, R. K. R.; Kuduva, S. S.; Reddy, D. S.; Xue, F.; Mak, T. C. W.; Nangia, A.; Desiraju, G. R. *Tetrahedron Lett.* **1998**, *39*, 913−916.

(7) Joachim, C.; Tang, H.; Moresco, F.; Rapenne, G.; Meyer, G. *Nanotechnology* **2002**, *13*, 330−335.

(8) Shirai, Y.; Morin, J. F.; Sasaki, T.; Guerrero, J. M.; Tour, J. M. *Chem. Soc. Rev.* **2006**, *35*, 1043−1055.

(9) Soldatov, D. V.; Moudrakovski, I. L.; Ratcliffe, C. I.; Dutrisac, R.; Ripmeester, J. A. *Chem. Mater.* **2003**, *15*, 4810−4818.

(10) Soldatov, D. V.; Tinnemans, P.; Enright, G. D.; Ratcliffe, C. I.; Diamente, P. R.; Ripmeester, J. A. . *Chem. Mater.* **2003**, *15*, 3826−3840.

(11) (a) Scudder, M.; Dance, I. *J. Chem. Soc., Dalton Trans.* **1998**, 329−344. (b) Scudder, M.; Dance, I. *Dalton* **2000**, 2909−2915. (c) Dance, I.; Scudder, M. *New J. Chem.* **1998**, *22*, 481−492. (d) Lacour, J.; Bernardinelli, G.; Russell, V.; Dance, I. *CrystEngComm* **2002**, *4*, 165−170.

(12) Karlen, S. D.; Kahn, S. I.; Garcia-Garibay, M. A. *Cryst. Growth Des.* **2005**, *5*, 53−55.

(13) (a) Dominguez, Z.; Khuong, T. A. V.; Sanrame, C. N.; Dang, H.; Nuñez, J. E.; Garcia-Garibay, M. A. *J. Am. Chem. Soc.* **2003**, *125*, 8827−8837. (b) Dominguez, Z.; Dang, H.; Strouse, J. M.; Garcia-Garibay, M. A. *J. Am. Chem. Soc.* **2002**, *124*, 7719−7727. (c) Santillan, R.; Karlen, S. D.; Dang, H.; Garcia-Garibay, M. A. *J. Mex. Chem. Soc.* **2008**, *52*, 125−129.

(14) Karlen, S. D.; Ortiz, R.; Chapman, O. L.; Garcia-Garibay, M. A. *J. Am. Chem. Soc.* **2005**, *127*, 6554−6555.

(15) O'Brien, Z. J.; Karlen, S. D.; Khan, S.; Garcia-Garibay, M. A. *J. Org. Chem.* **2010**, *75*, 2482−2491.

(16) Rodriguez-Molina, B.; Ochoa, M. E.; Farfán, N.; Santillan, R.; Garcia-Garibay, M. A. *J. Org. Chem.* **2009**, *74*, 8554−8565.

(17) Karlen, S. D.; Reyes, H.; Taylor, R. E.; Khan, S. I.; Hawthorne, M. F.; Garcia-Garibay, M. A. *Proc. Natl. Acad. Sci. U.S.A.* **2010**, *107*, 14973−14977.

(18) (a) Desiraju, G. R. Crystal Engineering: Solid State Supramolecular Synthesis. *Curr. Opin. Solid State Mater. Sci.* **1997**, *2*, 451−455. (b) Desiraju, G. R. Hydrogen Bridges in Crystal Engineering: Interaction without Borders. *Acc. Chem. Res.* **2002**, *35*, 565−573. (c) Desiraju, G. R. *Crystal Engineering: The Design of Organic Solids*; Elsevier: Amsterdam, 1989.

(19) Li, Q.; Rukavishnikov, A. V.; Petukhov, P. A.; Zaikova, T. O.; Keana, J. F. W. *Org. Lett.* **2002**, *4*, 3631−3634.

(20) Martin, N. H.; Allen, N. W., III; Moore, K. D.; Vo, L. *J. Mol. Struct.* **1998**, *454*, 161−166.

(21) Samples of **1** and **1**-d_{60} had identical crystallization behavior and their crystals appeared identical in all respects.

(22) Dance, I.; Scudder, M. *CrystEngComm* **2009**, *17*, 2233−2247.

(23) (a) Klebe, G.; Diederich, F. *Phil. Trans. R. Soc. London A* **1993**, *345*, 37−48. (b) Bludský, O.; Rubeš, M.; Soldán, P.; Nachtigall, P. *J. Chem. Phys.* **2008**, *128*, 114102.

(24) Boldog, I.; Lysenko, A. B.; Rusanov, E. B.; Chernega, A. N.; Domasevitch, K. V. *Acta Crystallogr.* **2009**, *C65*, 248−252.